Assessment of Slope Instability in Post-Wildfire Areas Using UAV-derived DTM and QGIS

Park J. W.[1], Koo S.[1], Jung Y. H.[2] and Kim S. S.[3*]

[1]Researcher, National Disaster Management Research Institute, Republic of Korea

[2]Senior Researcher, National Disaster Management Research Institute, Republic of Korea

[3]Senior Research Officer, National Disaster Management Research Institute, Republic of Korea

*sskim73@korea.kr   (*Corresponding author's email only)

Abstract *Wildfires significantly increase slope instability by inducing vegetation loss, topsoil erosion, and the formation of hydrophobic layers. When combined with rainfall, these changes can lead to large-scale mass movement phenomena such as landslides and debris flows within a short period. However, conventional slope instability assessments based on satellite imagery or field observations often lack the spatial resolution and accuracy required for detailed analysis. In contrast, UAV based photogrammetry enables the acquisition of high-spatial-resolution imagery and point cloud data at centimeter-level precision, allowing for fine-scale analysis of ground cover under the burned canopy. In this study, UAV photogrammetry were acquired using a state-of-the-art DJI Matrice 350 RTK drone equipped with a Zenmuse P1 optical camera. A Digital Elevation Model (DEM) was generated through DJI Terra software, and terrain analysis was conducted using QGIS. The analysis included slope mapping, and distance evaluation between slopes and residential structures. Considering the lack of vegetation in the post-fire environment, the results demonstrate that UAV-based photogrammetry can serve as an effective tool for high-spatial-resolution slope instability assessment. This approach presents a practical and scalable methodology that can contribute valuable data for post-wildfire disaster response and recovery planning.*

Keywords: Wildfire, UAV, Photogrammetry, Slope instability, GIS

Introduction

Wildfire frequency and scale are steadily increasing worldwide due to the combined effects of climate change, land-use alteration, and prolonged drought conditions(Akosah, 2025). Wildfires not only cause extensive destruction of vegetation and infrastructure within a short period of time but also induce significant changes in the physical and hydrological properties of hillslopes (Zhang, Y., 2024). Specifically, the removal of vegetation drastically reduces soil cohesion provided by roots, while the combustion of surface organic matter accelerates topsoil erosion (Akin, I., 2025). At the same time, the formation of a hydrophobic layer reduces the soil's infiltration capacity, leading to a rapid increase in surface runoff during subsequent rainfall events (Kim, S. W., 2019). These alterations can trigger large-scale geomorphic processes such as slope failures and debris flows (Francis, K. R., 2020). Consequently, post-wildfire slope instability poses a substantial threat to human lives, infrastructure, and ecological recovery, underscoring the critical need for early

and accurate assessment and prediction. For these reasons, conventional assessments of slope instability have primarily relied on satellite imagery analysis or field surveys (Choi, S. K., 2024). While satellite imagery provides broad spatial coverage, its spatial resolution—typically at the meter scale—makes it difficult to capture fine-scale topographic features that are critical for determining slope stability in mountainous terrain (Ruth, E. G., 2025). In contrast, field surveys offer high local accuracy but require significant manpower and time, and they often depend on qualitative judgments, limiting their ability to quantitatively measure and interpret complex geomorphic changes across extensive wildfire-affected areas (Lim, E. T., 2024). These limitations highlight the need for a new approach that can achieve both precision and efficiency. Against this backdrop, various methods have been explored to assess slope stability in wildfire-affected regions. Previous studies can largely be classified into two categories: precision deformation detection using high-resolution data, and large-scale susceptibility assessments of slope failures.

First, among the studies utilizing high-resolution data, Deligiannakis et al. (2021) quantitatively detected and monitored initial slope deformations immediately after a wildfire by comparing and integrating a DSM (Digital Surface Model) and point clouds derived from UAV-based SfM (Structure from Motion) photogrammetry with terrestrial LiDAR data. This study demonstrated that UAV-SfM is highly efficient in wildfire-affected areas where vegetation has been removed, and that it enables precise tracking of subtle deformations at specific locations. However, the research mainly focused on monitoring micro-deformations at selected sites, and the reliance on expensive instruments such as terrestrial LiDAR introduced limitations in terms of data acquisition and analytical efficiency.On the other hand, for large-scale assessments, Napoli et al. (2020) combined satellite-based EO (Earth Observation) data with machine learning techniques to evaluate slope failure susceptibility in wildfire-affected areas. While this approach is effective for analyzing broad spatial extents, the relatively low spatial resolution of satellite data limits its ability to capture localized fine-scale topographic and surface property changes. In other words, although it is useful for identifying large-scale hazard-prone zones, it is less suitable for diagnosing the detailed instability levels of individual slopes. In addition, Carabella et al. (2019) assessed post-wildfire landslide and debris-flow hazards through an integrated approach combining topographic, hydrological, and geological data with field investigations in the case of the 2017 Montagna del Morrone wildfire in Italy. This study effectively combined qualitative field observations with GIS-based topographic analysis for

hazard assessment; however, the integration process required substantial time and effort, raising concerns about efficiency. Collectively, these previous studies have made important contributions to post-wildfire slope stability assessment, while leaving room for approaches that can simultaneously satisfy the needs for local high-precision analysis, large-scale efficiency, and quantitative evaluation. In particular, integrated approaches capable of rapidly and quantitatively capturing slope characteristics that change immediately after wildfires, and of providing practical information for disaster mitigation, remain insufficient. The primary objective of this study is to precisely assess slope instability in wildfire-affected areas using UAV-based photogrammetry. High-resolution imagery was acquired with drones equipped with optical cameras, and a DEM (Digital Elevation Model) was generated through drone mapping software. Terrain analyses, including slope distribution and proximity to residential areas, were conducted in QGIS. By integrating UAV photogrammetry with GIS-based terrain analysis, this study aims to evaluate the potential for secondary hazards in post-wildfire landscapes and to provide quantitative data on topographic and geological risk factors, thereby supporting disaster response and recovery planning.

Methodology

a. Study Area

In March 2025, a large-scale wildfire occurred in Uiseong-gun, Gyeongsangbuk-do, South Korea. The fire, ignited by careless use of fire during grave visits, lasted for seven days (March 22–28) and burned 99,289 ha, resulting in 32 fatalities and property losses amounting to 794 million USD, making it the largest wildfire in Korean history. In particular, strong winds with a maximum speed of 25.4 m/s facilitated the spread of the fire across mountainous terrain, completely removing vegetation cover in steeply sloped areas. Consequently, the affected region became highly susceptible to secondary hazards such as landslides and debris flows due to the formation of hydrophobic layers and the potential for rapid increases in surface runoff during heavy rainfall events.

Accordingly, this study selected eight sites located in Yeongyang-gun and Yeongdeok-gun, Gyeongsangbuk-do, as case study areas requiring urgent slope instability assessment for nearby residential zones. These sites consist of steep slopes ranging from 24 m to 165 m in height, 137 m to 570 m in length, and 31° to 42° in gradient. The selected areas are considered high-risk zones where landslides and debris flows triggered by rainfall could

lead to significant damage to human lives and property. Detailed descriptions of the study sites are provided in Table 1.

Table 1: Geographical Information of Slopes in Wildfire-Affected Study Sites

Site Num.	Location [-]	Elevation [m]	Length [m]	Slope [°]
site 1		24	304	36
site 2		62	475	31
site 3	Yeongyang-gun, Gyeongsangbuk-do	63	137	42
site 4		130	570	36
site 5		165	161	35
site 6		121	428	42
site 7	Yeongdeok-gun, Gyeongsangbuk-do	71	250	37
site 8		61	423	42

b.   Data Acquisition

To acquire spatial information from the wildfire-affected areas, a DJI Matrice 350 RTK UAV (unmanned aerial vehicle) was employed. The UAV was equipped with a Zenmuse P1 optical camera with a 45 MP resolution, and high-precision trajectory data were simultaneously recorded using RTK (Real-Time Kinematic) corrections. Detailed specifications of the equipment are summarized in Table 2.

Table 2: Aircraft and Camera Sensor Specifications

Aircraft		Camera Sensor	
Category	Specs.	Category	Specs
Image		Image	
Model	Matrice 350 RTK	Model	Zenmuse P1
Dimensions	810×670×430 mm	Dimensions	198×166×129 mm
Weight	6.47 kg(With batteries)	Weight	800 g
Max Horizontal Speed	23 m/s	Sensor size	35.9×24 mm
Max Flight Time	55min.	Effective Pixels	45 MP
Hovering Accuracy	V ±0.1 m, H ± 0.3 m	Photo Size	8192×5460(3:2)
RTK Positioning Accuracy	V ±1.0 cm, H ±1.5 cm	Aperture Range	f/2.8~f/16

Flight missions were planned using DJI Pilot 2 software, taking into account the distribution of steep slopes in the wildfire-affected regions. Since the study sites included sections with steep gradients and significant terrain variability, flight paths were carefully designed to minimize image distortions caused by topographic relief and hazards from obstacles (Kim, D. H., 2023). In addition, UAV speed and altitude were adjusted to ensure the nominal GSD (Ground Sampling Distance) of the captured images. Flights were conducted over distances of 4.65–12.25 km at altitudes of 70–120 m and speeds of 9.5–13.7 m/s, balancing efficiency of data acquisition with image quality. A total of 479–1,010 images were captured, yielding a nominal GSD of 0.88–1.51 cm/pixel, depending on flight altitude and camera sensor resolution. Flight and imaging parameters are detailed in Table 3.

Table 3: Flight Operation Details for Drone-based Mapping

| Site Num.	Mapped Area [km²]	Flight Distance [km]	Flight Time [min]	Num. of Image [-]	Nominal GSD [cm/pixel]	Fligth Altitude [m]	Flight Speed [m/s]
site 1	0.06	4.65	9.48	540	0.88	70	9.5
site 2	0.23	10.28	15.13	686	1.51	120	13
site 3	0.16	8.55	14.95	743	1.26	100	12
site 4	0.25	12.25	19.2	1010	1.26	100	12.5
site 5	0.09	5.05	8.52	479	1.26	100	13.7
site 6	0.19	9.87	15.18	854	1.26	100	13.7
site 7	0.11	7.26	140.68	766	1.01	80	10
site 8	0.11	6.87	12.9	674	1.01	80	10

c.   Data Processing
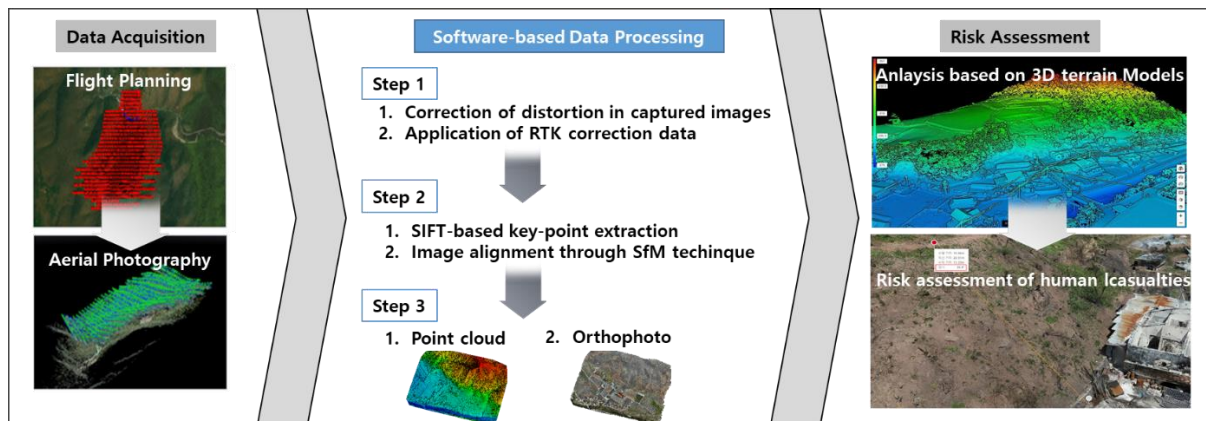
Figure 1: Data Processing Workflow of This Study

Figure 1 illustrates the workflow for processing UAV-derived imagery using DJI Terra software, encompassing all stages from data acquisition to risk assessment. Initially,

geometric distortions introduced by the camera and lens are corrected, and aerial images are georeferenced to align with a ground coordinate system, ensuring the fundamental accuracy required for subsequent image registration. Key-points are extracted and matched across images to estimate camera poses and generate a sparse 3D point cloud, forming the geometric framework of the entire scene. Finally, dense three-dimensional surfaces, including DSM (Digital Surface Model) and DTM (Digital Terrain Model), as well as geometrically corrected orthophotos, are produced for terrain analysis. The processed DEM were subsequently utilized in QGIS to assess slope distributions and proximity to residential areas.

Results

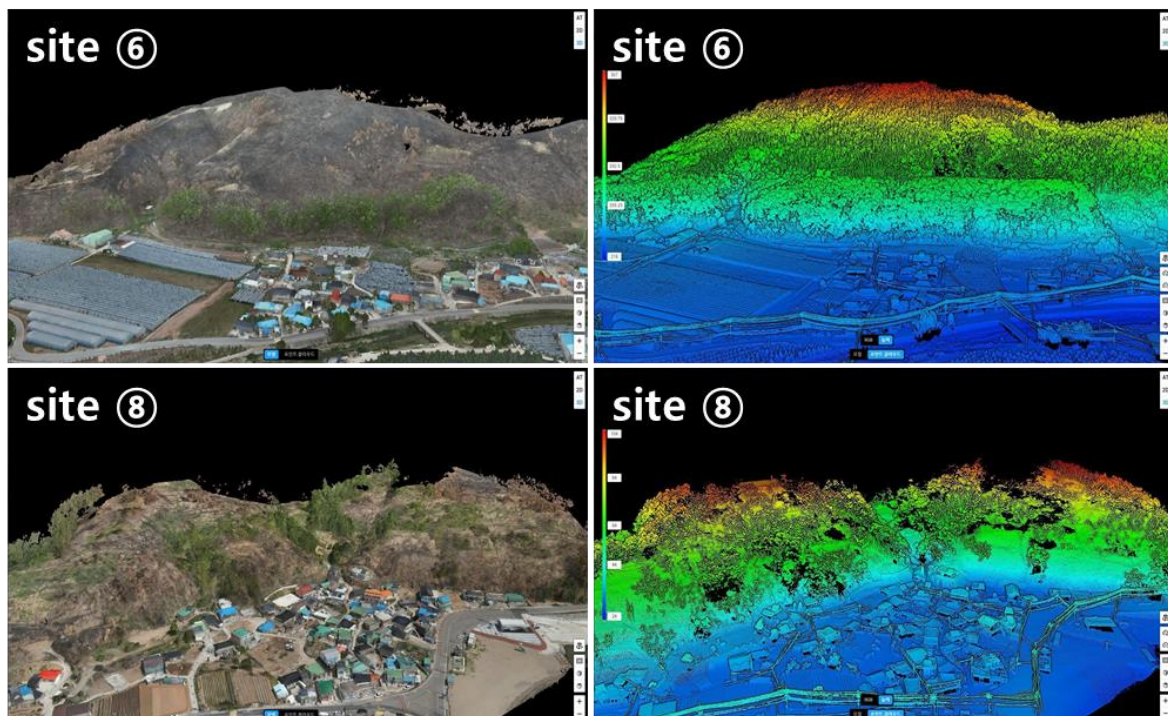**a.   Generation of High-Resolution Terrain Data**

Figure 2: Results of 3D Model Generation Based on Orthophotos(left) and Point Cloud(right)

Figure 2 presents the orthophotos and point cloud-based 3D models for Site 6, which generated the highest number of point clouds, and Site 8, which generated the fewest. The orthophotos visually confirm that the slope morphology of the wildfire-affected areas was accurately reproduced, while the point clouds allow height variations to be observed through color differentiation. Notably, by generating DEMs in areas where the canopy had

been removed by the wildfire, the terrain morphology—previously obscured by forests or vegetation—could be precisely reconstructed.

The number of points in the generated point clouds ranged from approximately 240 million to 440 million. The resulting models were evaluated based on GSD (Ground Sampling Distance) and RMSE (Root Mean Square Error). The models exhibited GSD values of 0.804−1.288 cm/pixel and RMSE values of 0.022–0.129 m. Validation at Site 5 yielded an RMSE of 0.129 m, which was 0.104 m higher than the average. This discrepancy was attributed to Site 5 generating 115,104 fewer key points for image matching compared to the average of other sites, resulting in a higher RMSE during the bundle adjustment (BA) process. Consequently, Site 5 was excluded from further analysis, and it was confirmed that the remaining sites provided sufficient spatial resolution to conduct precise terrain analyses of the wildfire-affected areas. Detailed results of the model quality assessment are summarized in Table 4.

Table 4: Results of Modeling Quality Assessment

Site Num.	Num. of Point Cloud	Num. of Key-point	GSD	RMSE
	[-]	[-]	[cm/px]	[m]
site 1	243,657,872	216,912	0.804	0.023
site 2	339,832,245	299,498	1.288	0.028
site 3	306,787,439	280,516	1.16	0.026
site 4	415,277,132	363,362	1.203	0.03
site 5	243,997,158	163,807	1.231	0.129
site 6	447,794,496	327,955	1.201	0.023
site 7	212,150,312	244,058	0.917	0.025
site 8	202,038,657	220,074	0.961	0.022

b.   Distance between Slopes and Adjacent Residential Areas

Figure 3: Assessment of Distance between Slopes and Adjacent Residential Areas

Figure 3 presents the results of secondary hazard assessment based on the distances between wildfire-affected slopes and nearby residential areas for Sites 6 and 8. The assessment criteria were adapted from established methods used in natural slope disaster risk evaluations, where regions with steep slopes located within half the slope height from adjacent structures were designated as potential zones for debris impact at the slope base. The measured distances for the study sites were 12 m, 31 m, 34 m, 65 m, 60.5 m, 35.5 m, and 30.5 m, respectively. It was determined that 55 households are situated within these high-risk zones, indicating a significant potential for direct threat to the villages in the event of debris flows during future rainfall events.

c.   Slope Analysis

Figure 4 presents the results of slope gradient analysis for Sites 6 and 8, conducted by importing DEM into QGIS. To evaluate slope stability and the potential for secondary hazards, slopes were categorized into three classes: slopes below 30°(no color), 30°–40° marked in yellow, and slopes exceeding 40° marked in red. The measured slope gradients near residential areas were 35.8°, 30.7°, 41.7°, 36.2°, 42.0°, 36.7°, and 42.2° across the study sites, with an average slope of 37.9°. Except for Site 2, all other sites exhibited slopes greater than 34°, meeting the criteria for steep slopes as defined by the Enforcement Decree of the Act on the Prevention and Management of Steep Slope Disasters. Consequently, these areas are considered to require legal-level disaster prevention and management measures.
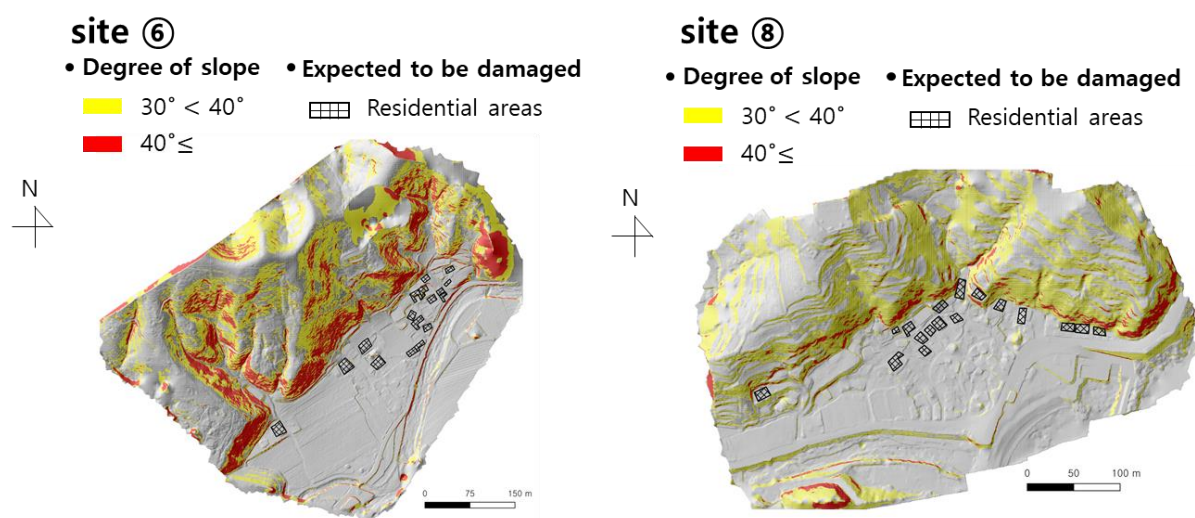

Figure 4: Results of Slope Hazard Analysis for Residential Areas Based on DEM

Discussion

a.   Advantages of UAV-based Analysis

The UAV photogrammetry-based assessment of slope instability conducted in this study demonstrated several advantages compared to conventional satellite imagery analysis and field surveys. First, the data acquired by UAVs provided an average GSD 1.18 cm/pixel, allowing detailed identification of small-scale terrain changes and the distribution of affected trees. Such fine-scale information is difficult to obtain from satellite imagery with meter-level resolution. Second, UAVs can be operated flexibly in mountainous terrain that is otherwise difficult to access, enabling rapid coverage of extensive wildfire-affected areas. Third, the high precision of the data, achieved through RTK-based positional correction, provided reliable inputs for subsequent GIS(Geographic Information System) analyses. These advantages highlight the potential of UAV-based approaches as effective tools for decision-making, particularly in urgent post-wildfire situations.

b.   Comparison with Existing Studies

Previous studies on post-wildfire slope instability have primarily relied on satellite-based land cover change analysis or field-based soil surveys. However, these approaches are limited in terms of spatial coverage and fine-scale terrain analysis. While satellite imagery is useful for obtaining a general overview of the affected area, it is insufficient for assessing localized risk factors such as slope distribution or the potential occurrence of debris flows in valleys. In contrast, the UAV-based analysis employed in this study addresses these limitations, allowing direct extraction of detailed terrain features and damage characteristics, thereby providing a distinctive advantage.

c.   Limitations and Constraints

Nevertheless, this study has several limitations. First, UAV-based optical sensors cannot directly capture terrain information beneath tree canopies, which may result in reduced accuracy of terrain models in areas where vegetation remains. Second, UAV operations are highly influenced by weather conditions; strong winds, rain, and fog can directly constrain flight safety and image quality. Third, when the survey area is extensive, the limited battery capacity and flight time of UAVs make it difficult to cover the entire region in a single mission. Therefore, for long-term monitoring over large areas, integration with satellite data or UAV-LiDAR-based data acquisition is recommended in regions with remaining vegetation.

Conclusion

This study proposed a methodology combining UAV-derived photogrammetry and GIS analysis for the precise assessment of slope instability in post-wildfire areas. High-resolution imagery was acquired in mountainous wildfire-affected regions using a DJI Matrice 350 RTK UAV equipped with a Zenmuse P1 optical camera, from which orthophotos and DEM were generated. The analysis revealed that a substantial portion of the study area consisted of slopes steeper than 30°, with some sections located in close proximity to residential areas, indicating high potential risk. Valleys were identified as pathways with a high likelihood of debris flows during intense rainfall, and the distribution of affected trees was recognized as a key factor contributing to slope instability. These results demonstrate that UAVs can provide significantly higher spatial resolution and accuracy than conventional satellite imagery or field-based approaches, making them effective tools for post-wildfire slope stability assessment. In particular, UAV-based methods enable rapid and efficient data acquisition and precise analysis of terrain-related risk factors in urgent post-fire situations, offering substantial practical value. However, optical sensor-based UAV analysis is limited in capturing terrain beneath the canopy and is subject to weather conditions and flight time constraints. Future studies should consider integrating satellite imagery or employing UAV-LiDAR-based analyses. Moreover, through overlay analyses, a more precise and comprehensive framework for assessing post-wildfire slope instability can be established.

References

Akosah, S., & Gratchev, I. (2025). Systematic review of post-wildfire landslides. *GeoHazards,* 6(1), 12.

Zhang, Y., Liu, H., & Sun, Z. (2024). Post-wildfire boreal forest vegetation cover change: Mapping via multi-source fusion. *International Journal of Applied Earth Observation and Geoinformation,* 125, 103612.

Choi, S. K., Kim, H. J., & Lee, D. Y. (2024). Multi-source remote sensing-based landslide investigation. *Remote Sensing Applications,* 8(1), 101–118.

Akin, I., Gomez, J., & Stevens, M. (2025). Reconnaissance of the geotechnical and infrastructure impacts of Los Angeles wildfires (GEER report). *Geotechnical Extreme Events Reconnaissance Reports,* 43, 1–56.

S. W. Kim, M. S. Kim, H. U. An, K. W. Chun, H. J. Oh, Y. Onda, Influence of subsurface flow by Lidar DEMs and physical soil strength considering a simple hydrologic concept for shallow landslide instability mapping, *Catena,* 182, 104137.

Francis K. Rengers I Luke A. McGuire I Nina S. Oakley I Jason W. Kean I Dennis M. Staley I Hui Tang, Landslides after wildfire: initiation, magnitude, and mobility, *Landslides,* 17, 2631–2641.

Xie, C., Liu, T., Xu, W., Chen, X., & Chen, J. (2023). Remote sensing for wildfire mapping: A comprehensive review of advances, platforms, and algorithms. *Fire,* 6(2), 75. https://doi.org/10.3390/fire6020075

Lim, E., Kim, J., Park, S., & Lee, H. (2024). Investigation and analysis of landslide damage caused by heavy rainfall using drone mapping. *Korean Journal of Remote Sensing,* 40(6), 1347–1357.

Deligiannakis, G., Pallikarakis, A., Papanikolaou, I., Alexiou, S., & Reicherter, K. (2021). Detecting and monitoring early post-fire sliding phenomena using UAV-SfM photogrammetry and t-LiDAR-derived point clouds. *Fire,* 4(4), 87.

Di Napoli, M., & Santangelo, M. (2020). Landslide susceptibility assessment of wildfire burnt areas through earth-observation techniques and a machine learning-based approach. *Remote Sensing,* 12(15), 2505.

Carabella, C., Miccadei, E., Paglia, G., & Sciarra, N. (2019). Post-wildfire landslide hazard assessment: The case of the 2017 Montagna del Morrone fire (Central Apennines, Italy). *Geosciences,* 9(4), 175.

Kim, H., Lee, J., & Park, K. (2023). Risk assessment and analysis of steep slope hazards using drone and terrestrial LiDAR. *Journal of the Korean Society of Hazard Mitigation,* 23(5), 101–112.